Publications

Available Online

J. Sci. Res. **14** (3), 813-830 (2022)

JOURNAL OF SCIENTIFIC RESEARCH

www.banglajol.info/index.php/JSR

Interpretation of Acousting Sounding Records with Meterological Parameters and Ventilation Coefficient Over Delhi

P. Singh[1,2], K. Soni[2,3*], A. S. Nair[1,2], N. Kumar[3], R. Sharma[1,2]

[1]CSIR-National Physical Laboratory, New Delhi, India

[2]Academy of Scientific and Innovative Research (AcSIR), Ghaziabad-201002, India

[3]CSIR-Advanced Materials and Process Research, Madhya Pradesh, India

Received 18 February 2022, accepted in final revised form 2 June 2022

Abstract

Atmospheric Boundary Layer (ABL) height is an important parameter in defining the Ventilation Coefficient (VC) of any area. In this work, SODAR (Sound Detection and Ranging) observed data of different echograms for the year 2020 has been used for structure identification. The interpretation of ecograms is often not straight-forward. In this paper, an interpretation of different echograms along with meteorological parameters over Delhi is described. The ecogram structures were interpreted along with VC analysis. It is observed from the structures that during foggy days, VC values vary from day to day in the winter, with daily maximum values occurring between 13:00 and 15:00 h. The daytime values varied significantly from sunrise to sunset, while the night-time values remained relatively stable (200 m^2/s). However, due to fog diurnal variation from 16:00 h to 11:00 h, that is from evening to all night and then the next morning until 12:00 h, the atmospheric condition remained stable. At maximal wind speeds, a maximum VC of 1600 m^2/s (at 12:00 h) was observed during extended fumigation. With minimal wind speeds and ABL height, a minimum VC of 100 m^2/s (at 20:00 h) was observed. However, both VCs were smaller than the optimal VC for 6000 m^2/s safe dispersion.

Keywords: SODAR; Convection; Inversion; Atmosperic boundary layer; Stable layer; Ecogram; Ventilation coefficient.

doi: http://dx.doi.org/10.3329/jsr.v14i3.58317 J. Sci. Res. **14** (3), 813-830 (2022)

1. Introduction

All major environmental and meteorological factors are directly or indirectly impacted by Atmospheric Boundary Layer (ABL) structure and height, which is the lowermost layer of troposphere [1-9]. ABL height, defined here as the height to which airborne pollutants are mixed by the turbulent atmosphere, is an important and useful parameter in dispersion studies. Under convective conditions during the day ABL height is usually given by the height of the base of a capping inversion. During stable conditions at night, the ABL

* *Corresponding author*: 2006.kirti@gmail.com

height is usually taken to be the depth of the shallow turbulent region adjacent to the ground. Change in pollutant concentration and dispersion, wind velocity and vertical change in momentum, heat, gaseous constituents and aerosols are directly affected by change in height of ABL or more precisely, ABL is a main link between atmosphere and earth's surface and plays a major role in influencing atmospheric environment and human life [9-12]. ABL structure is constantly changes in time and space with respect to change in mountain structure, different seasons, change in weather condition and during different hours of day. ABL height may change from less than 100 m to several thousand meters [4]. Knowledge of change in ABL is also important for weather forecasting, environmental policy planning and to gain knowledge about turbulence and dispersion of pollutant [3,5,13].

There are numerous techniques for ABL height determination. Major technique includes direct measurement such as Tethered balloon, Radiosonde and Remote sensing techniques such as Lidar, Doppler Radar and Sodar [4,6,14,15]. Among all these, SODAR is a valuable and significant instrument for ABL height determination upto 3 km with real time and good space resolution capability [16-19]. Since the last 40-years SODAR technique has been developed to a very useful tool for ABL investigation. There is a lot of methods for remote sensing of the lower atmosphere using lasers or radio waves, but sound waves have especially been favoured to become a frequently used technique all over the world due to the low cost needed for its instrumentation and long-time maintenance.

For the present study, monostatic SODAR instrument has been used. The whole system is developed and designed indigenously. SODAR provides a pictorial view of ABL height in the form of echograms [9]. Also, sensors for different meteorological parameters such as wind speed, wind direction, relative humidity and temperature have been installed along with SODAR. ABL height of any area mainly depends upon prevailing meteorological conditions of that area. Structure and height keep on changing in Echograms during different seasons and also during different time of a day and that can be used for study of hourly variation in ABL height.

In the present study, echograms for a year 2020 has been used and described. Echogram interpretation requires knowledge of local and boundary layer metrology, and the scattering of sound by atmospheric processes. Therefore, it is not usually a simple task and, in many instances, a high degree of subjective judgement may still be needed. The Acoustic Sounder (SODAR) can be very useful for the continuous monitoring of the atmosphere's thermal structures. The structure of the Sodar echogram is the characteristic of the time season and the ambient micrometeorological conditions of the lower atmosphere. These conditions influence the tropospheric propagation characteristics of electromagnetic waves, as well as posing a threat to aviation and air pollution. As a result, the Sodar echogram's distinctive information serves as an index for such scenarios. The many types of detected structures on the Sodar echograms have been described with this in mind.

2. Data and Meteorology

Data in the form of echograms is produced by SODAR at CSIR-National Physical Laboratory (NPL), New Delhi. Echograms are produced as a result of turbulence in the lower atmosphere [20,21]. This is the main factor responsible for pollutant dispersion. Measurement of the height of the thermal plume during the daytime and shear echoes during the night is used for the calculation of ABL height.

Generally, SODAR sensitivity is impacted by daytime activity as compared to night-time, which results in a decrease in its probing range. The daytime ABL height is always an underrated value and needs to be calculated by using an empirical equation developed by using the Holzworth model using radiosonde data [22–24].

$$Y=4.24X+95$$

Y is the ABL height (m) and X is the depth of the thermal plume measured by SODAR.

3. Result and Discussion

It is very important to measure the wind speed and temperature structure in the boundary layer for studying the air-sea interaction and air pollution [25,26]. Low level wind shear directly impacts airplane flying safety and missile launching [27-30]. Therefore, CSIR-NPL developed a new SODAR system. It may be used for the study of the structure of ABL over land and ocean. It is also applied in real-time monitoring of environmental protection and nowcasting of military and civil aviation. The main advantage of the CSIR-NPL designed/developed SODAR system is that it has a weather sensor mounted at the height of the SODAR and the software is also designed in such a way that the ABL height and meteorological parameters like temperature, relative humidity, and wind speed/wind direction can be compared simultaneously in a single window [21]. As these parameters are the main variables that affect the ABL height, for the first time, different structures of SODAR are compared and analysed at each hour along with meteorological parameters in a single window.

3.1. *Assessment of convective boundary layer for day time*

It is necessary to define convection in order to ensure that in cases where the ground based thermal plumes are not distinct, the ABL height inferred is due to the effects of solar heating and thereby meets the description "convective" [31]. The daytime instability of the convective boundary layer is usually capped by an elevated stable layer and so is considered to extend from the ground to the base of the elevated inversion. It increases in the morning due to the sun's heating of the earth's surface, peaks around midday, and then declines in the afternoon (Figs. 1 and 2).

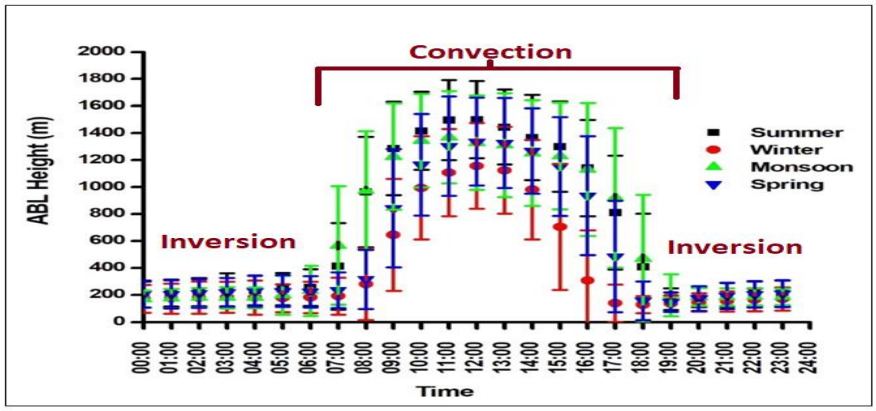

Fig. 1**.** Monthly average temporal and seasonal (Summer, Winter, Monsoon and Spring) variation of ABL height over Delhi.

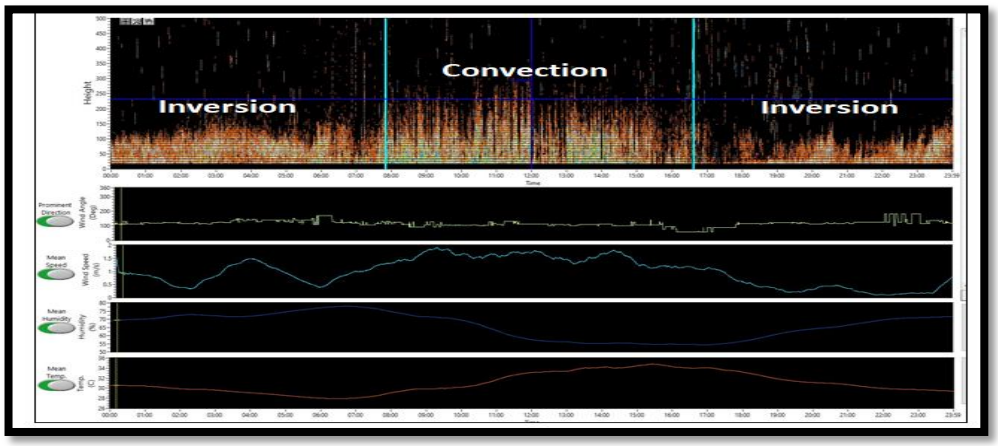

Fig. 2. ABL height record taken during 24 h.

The record starts at 00.00 h on 23/09/2020 and continues up to 23:59. After 0700 h the thermals states appearing slowly and reaching up to 300 m. The thermals start disappears after 17:30 h. It is clear from Fig. 2 that maximum height is observed when temperature increases and relative humidity (RH) decreases and low height is found when temperature decreases and RH increases. High wind speed also plays a major role for the enhancement of mixing height. Solar heating and nocturnal cooling of the surface of the earth and friction between the flow and the surface are responsible for developing a surface layer called the ABL. Besides thermal turbulence, mechanical influence also remains present in this layer.

Plumes generally denote unstable conditions where the degree of instability increases with height above ground. Under the convection, SODAR represents thermal plumes (Fig. 3). The pressure on the ground falls as a thermal plume rises, while the impinging air mass causes the pressure to rise. As a result, pressure fluctuations in both positive and negative directions are linked to the thermal plumes. Fig. 3 shows the hourly variation of thermal plumes on a clear, sunny, and calm day (wind speed is around 1 m/s).

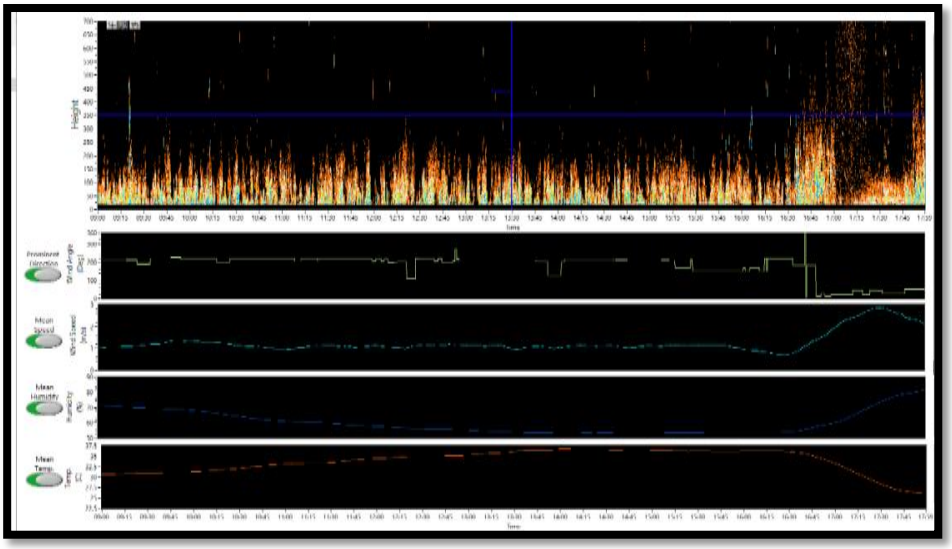

Fig. 3. Thermal plumes.

3.2. *Assesment of nocturnal boundary layer*

The nocturnal stable boundary layer contiguous with the surface of the earth is characterised by a potential temperature gradient and is generally formed only during clear nights over land. It forms shortly after sundown, grows continuously until early morning, and dissipates after sunrise when a thermally convective atmosphere develops near the ground surface [31,34]. Radiative cooling, shear generated turbulence, and horizontal advection are considered to be responsible for the growth of the nocturnal boundary layer, while the winds may modify the structure of the boundary layer [33].

Ground-based inversions are reported to emerge during the night due to radiative cooling of the earth's surface and often extend up to a height of 100 to 200 m [15]. The ideal conditions for the development of ground based inversions are long nights, clear sky conditions, and relatively dry and calm air. These inversions occur in both hilly and flat terrain. They are usually strongest in the valley of hilly terrain. Fig. 4 shows the development of a ground-based inversion on a clear night under very light wind conditions. It shows the growth of inversion with time. Normally, the formation of ground

based inversions is a nighttime phenomenon, but they may occur at any time of the day due to cloudiness. The Ventilation Coefficient (VC) during the night is very low, between 50-180 m²/s.

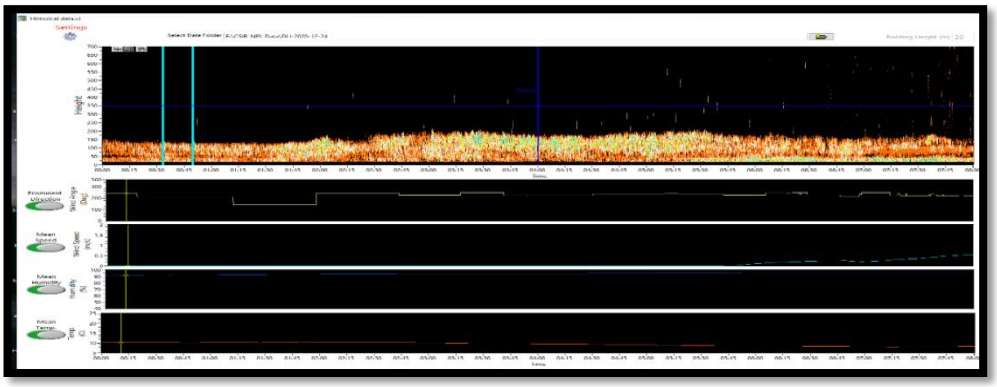

Fig. 4. Night time inversion layer.

3.3. *Assesment of elevated layer*

The next type of inversion is elevated layers. Subsidence and advection associated with the passage of a cold front in uniform and complicated terrain, cold-air outflows from local thunder storms, and drainage winds in the proximity of mountain ranges are all factors that contribute to the production of raised layers. As seen in Fig. 5, an elevated layer is essentially a suspended layer in the atmosphere. The creation of elevated strata appears to be mostly a nighttime event. They usually occur with a ground-based inversion [22]. The occurrence of elevated layers without any other temperature structure is very rare. Once produced, the raised layers last for several hours. Rising inversions are the most common way in which inversions dissipate. The nighttime stable layer does not dissipate soon after sunrise. The majority of the thermal energy is used to heat the earth after ground dawn, which warms the stable layer and pushes it upwards. The inversion's thickness decreases over time and eventually dissipates at a specific height, depending on the inversion's strength and daily weather conditions [23].

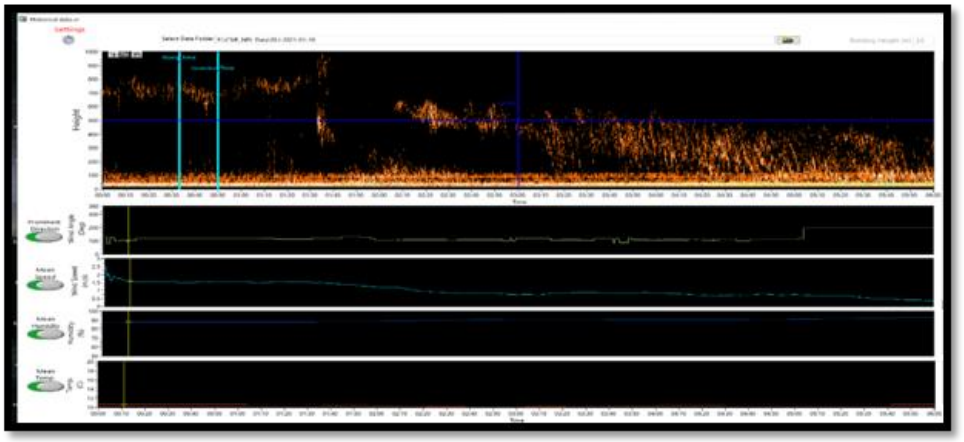

Fig. 5. Elevated layer.

3.4. *Assesment of fog layer*

During winter months, dense fog conditions, causing poor visibility, prevail continuously for a few days over the entire north-eastern region of India. Such fog conditions are said to be associated with synoptic weather conditions caused by eastward cyclonic circulations. Fog formation within a shallow surface layer at a depth of a few meters is commonly observed during winter nights due to the radiational ground cooling under calm, clear skies with fairly high relative humidity conditions [32]. Such fogs normally disperse within 1 to 3 h after sun rise but at times they may also become extensive vertically under increased influence of local turbulence and favorable meteorological conditions of synoptic origin associated with the advection of warm moist air into the colder region. In Figs. 6 to 9, SODAR observations pertaining to such a case of a foggy boundary layer have been examined in the light of local and synoptic meteorological conditions to identify the anomalies in thermal structure and their impact on the visibility conditions. The events belong to the period of December 2020 to January 2021. As seen in echograms (Figs. 6–9), a low-lying elevated layer, in addition to the ground based Stable Boundary Layer (SBL), was mapped in accordance with the occurrence of fog. The elevated layer subsequently persisted throughout the day for the whole of the foggy period, but its temporary disappearance during the early evening hours when the SBL was developing after the dissipation of the daytime convective thermal plumes. During the daytime, the elevated layer was seen to ascend and descend in accordance with the rise and fall of the convective boundary layer height in association with the increase and decrease of surface temperature due to solar heating of the ground [32].

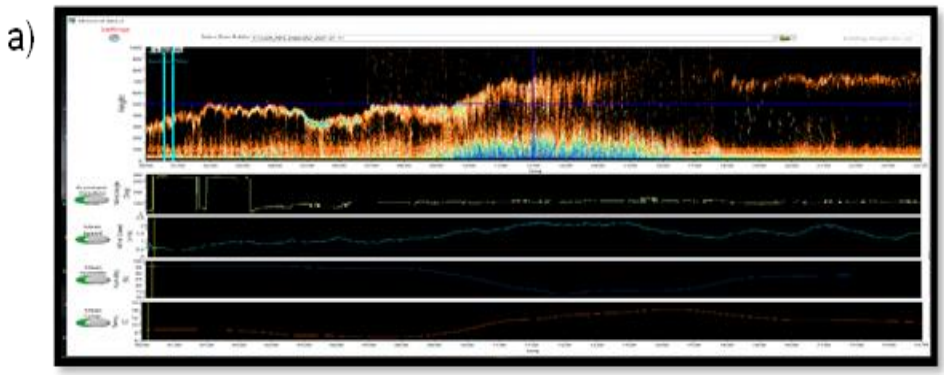

Fig. 6. (a) 24 h fog.

Due to fog conditions, the VC values were low for a longer time duration during the day hours. In winter, fog conditions prevail in the inversion condition for day and night most of the hours, except for a few hours in the afternoon. It is observed that VC values (Fig. 6b) vary from day to day during winter, with daily maximum values occurring in the late afternoon between 13:00 to 15:00 h. The daytime values varied significantly from sunrise to sunset, the nighttime values were relatively stable (< 200 m²/s), but due to fog diurnal variation from 16:00 h to 11:00 h that is from evening to all night then next morning till 12:00 h, there is stable atmospheric condition due to fog layer.

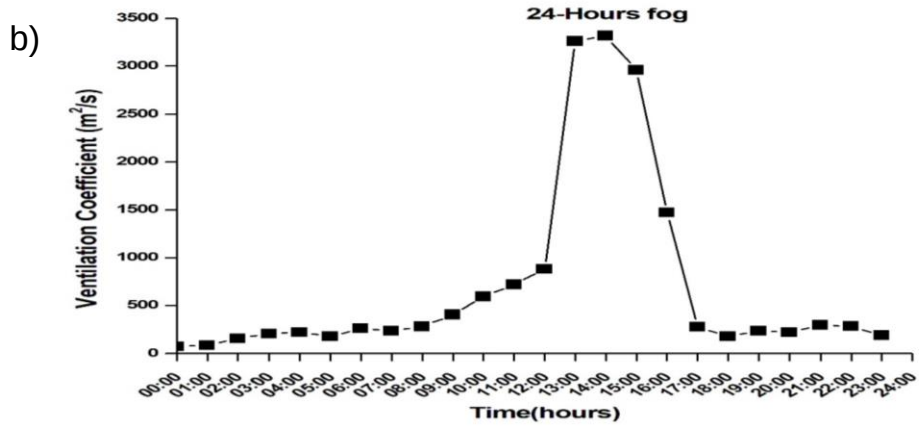

Fig. 6. (b) VC during all day-night fog.

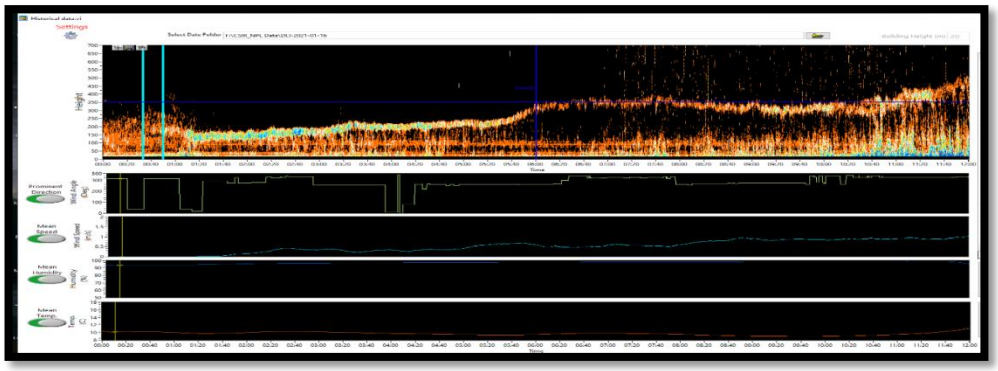

Fig. 7. Fog with thermal plumes early morning and day hours.

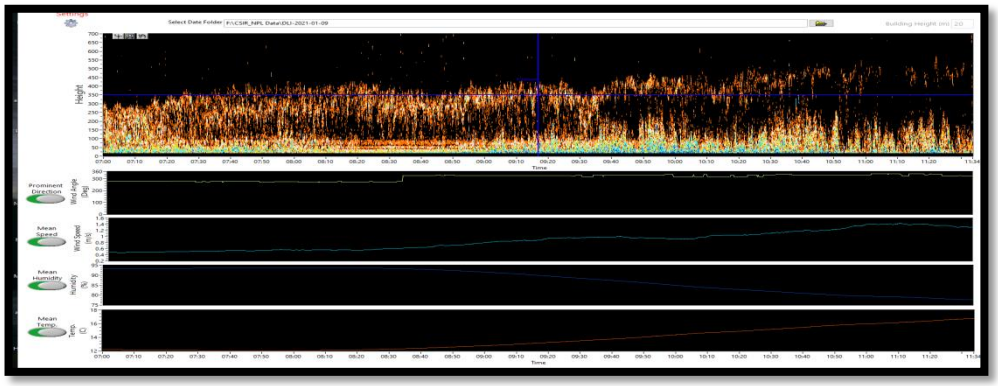

Fig. 8. Morning hours with fog layer.

a)

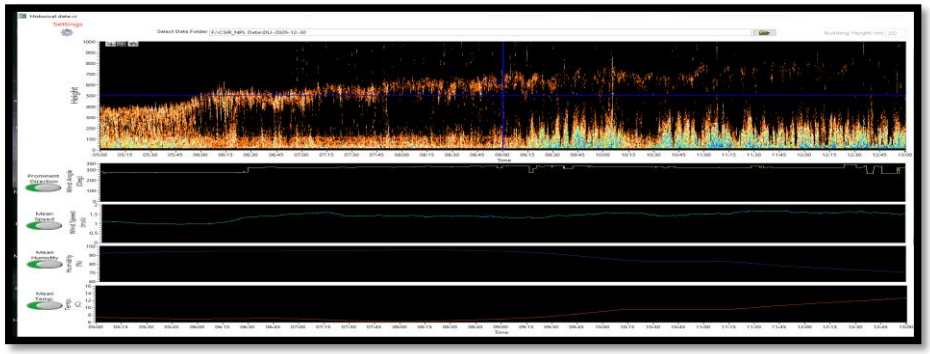

Fig. 9. (a) Fog layer with thermal plumes.

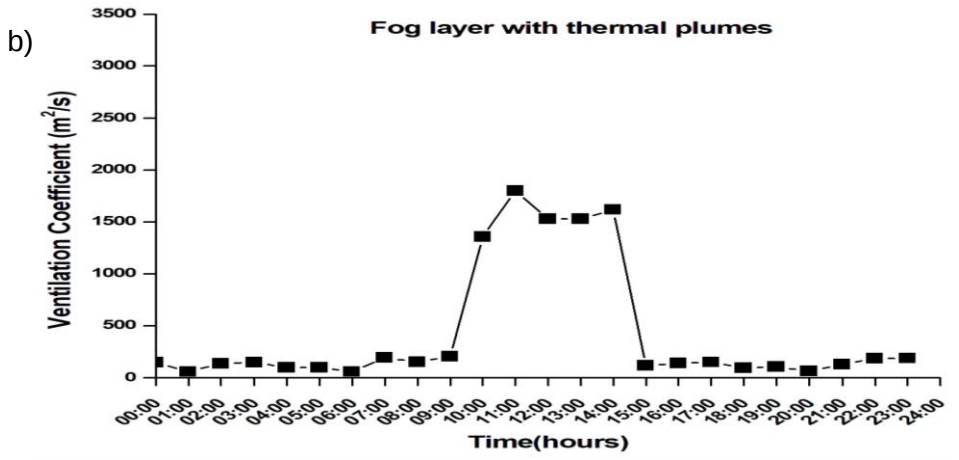

Fig. 9. (b) VC during Thermal plumes along with fog.

When the fog layer formed for small duration of time then thermal plume also occur in day time so the VC values increase due to thermal plumes in afternoon (Fig. 9b).

3.5. *Assessment of fumigation*

The morning rising layer with thermal echoes underneath represents fumigation conditions. This is the most dangerous plume. All contaminants can come down to ground level. When atmospheric conditions are steady above the plume but unstable below, this occurs. This usually occurs after the sun has warmed the atmosphere, turning a nighttime fanning plume into fumigation for about 0.5 h [33].

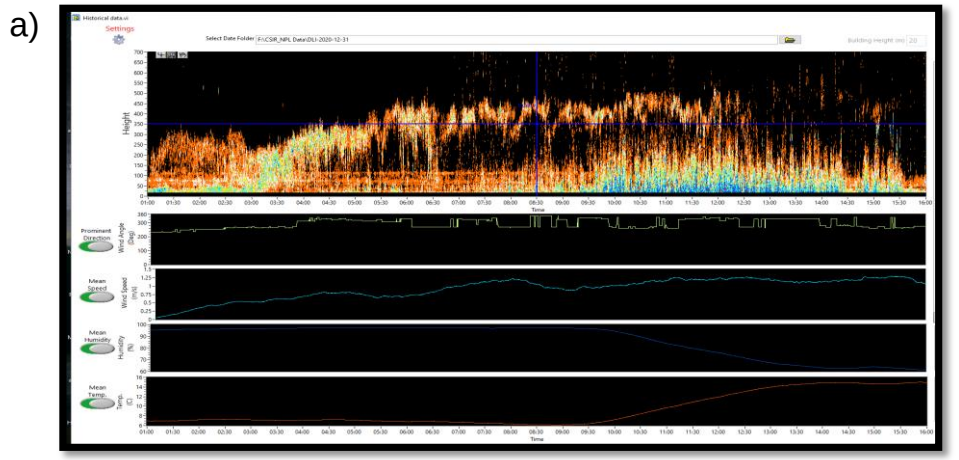

Fig. 10. (a) Prolonged fumigation.

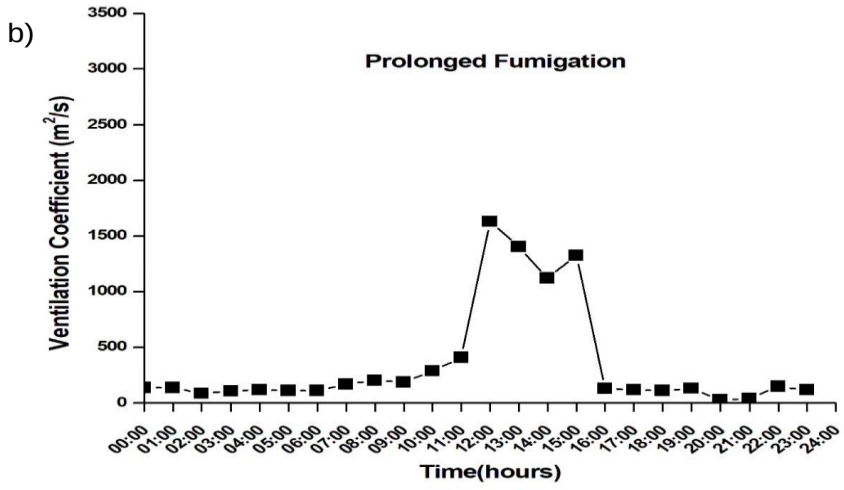

Fig. 10. (b) Diurnal variation of VC during prolonged fumigation condition.

Graphs of maximum VCs for maximum and minimum wind speed, and ABL heights against time during prolonged fumigation conditions are shown in Figs. 10 (a,b). It was found that wind speeds, ABL height, and VC values were lower during late night and early morning periods. During prolonged fumigation conditions, a maximum VC of 1600 m^2/s (at 12:00 h) (Fig. 10b) was observed with maximum wind speeds. A minimum VC of 100 m^2/s (at 20:00 h) was noticed with minimum wind speeds and ABL height. However, both the VCs were less than the favorable VC for safe dispersion of 6000 m^2/s.

3.6. *Assessment of rising layer*

The rising layer acting as a lid on the development of thermal plumes in the morning hours marks a typical signature of the infrasonic pressure fluctuations as shown in Fig. 11. The depression in pressure is caused when the rising layer gets eroded fast, thus suddenly removing the lid on the thermals below the inversion. This phenomenon suddenly reduces the pressure on the ground and is recorded as a positive sign of the sudden growth or dissipation of the rising layer. However, when the growth is gradual and the inversion breaks slowly, the typical signature may not appear [12,14]. In the sense of the detection of the dynamics of the rising layer, acoustic sounding is positively a better technique than others. Fig. 11b shows the variation of VC along with temperature, wind, and ABL height. Maximum daily average value of 2000 m^2/s observed during this day.

a)

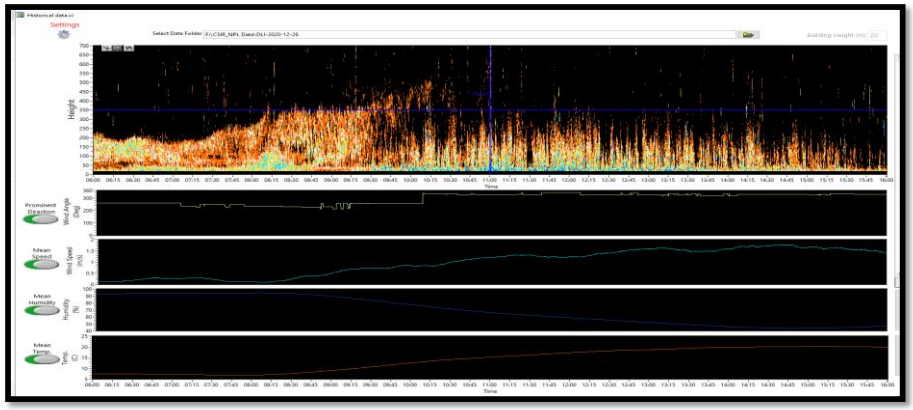

Fig. 11. (a) Typical signature of rising layer.

b)

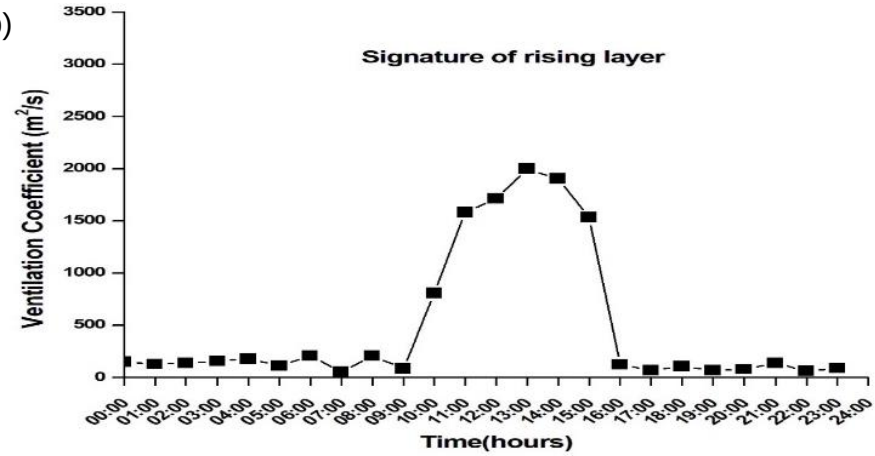

Fig. 11. (b) Diurnal variation of VC along with rising layer.

3.7. *Assessment of multilayer structure*

Multilayer observed under clear weather conditions has the presence of both wind shear and thermal inhomogeneity. However, on days of frontal disturbances, the forward scattered structures show higher intensity as compared to back scattered echoes, indicating the dominance of wind shear under such conditions [12]. Figs. 12(a,b,c) represent the different multilayer structures and variation of VC during multilayer structures respectively.

a)

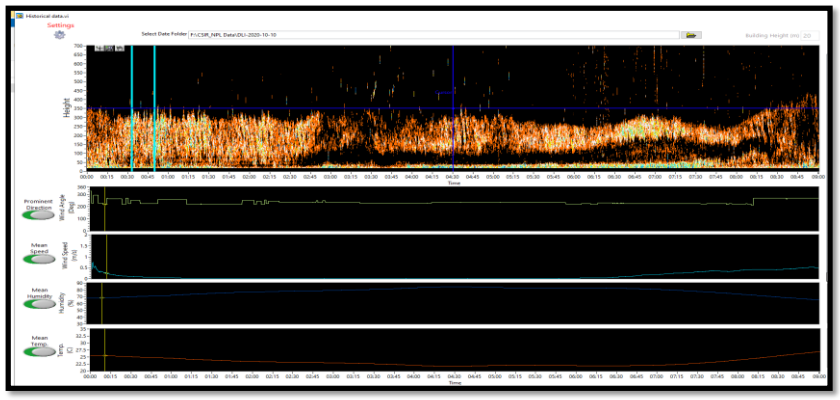

Fig. 12. (a) Multilayer structure.

b)

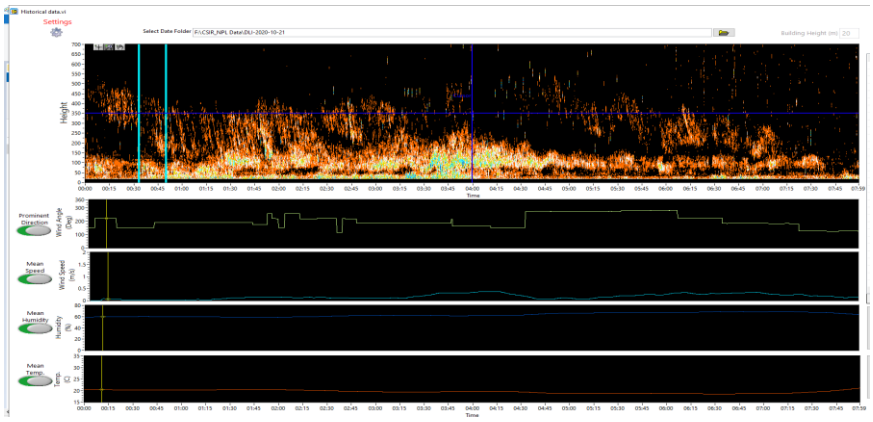

Fig. 12. (b) Multilayer structure.

c)

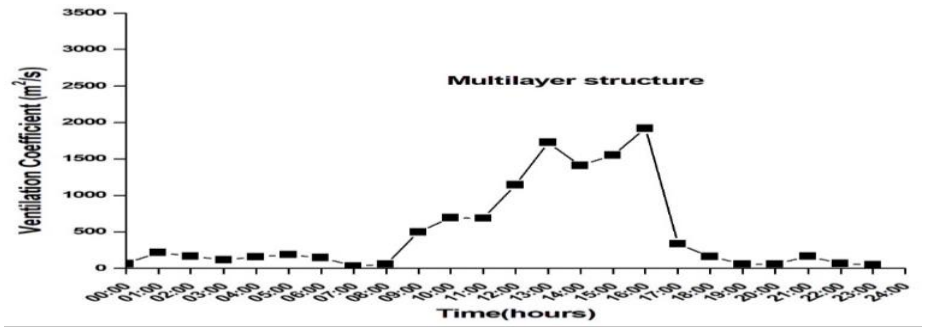

Fig. 12. (c) VC variation during multilayer structure.

3.8. *Assessment of wind shear of the ABL*

These are predominantly horizontal echo regions, which denote the turbulent interface between two layers of air (Fig. 13). The turbulence is powered mechanically by the wind shear, which dominates over the stable temperature profile effect. This wind driven echo region may be shallow or deep and may mark a mixing region aloft or indicate the boundary layer region at the surface. Echoes from horizontally stratified layers usually contain evidence of organized wave structure, indicating a stable lapse rate.

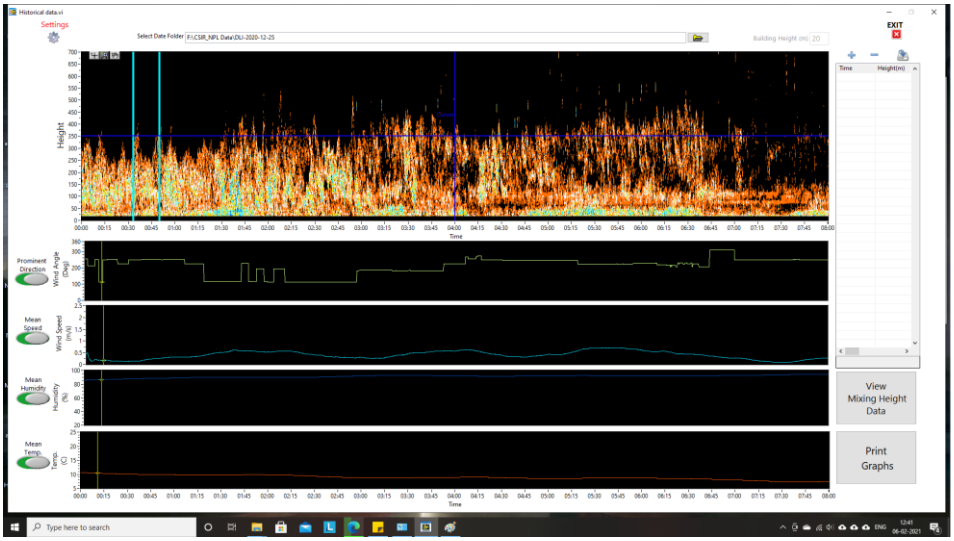

Fig. 13. Shear echoes.

Wind shear [14,34] is recognized to be of two types. It may be associated with large scale frontal or inversion surfaces and usually occurs above the ground with little or no surface manifestation. Alternately, it may be related to the fronts that result from cold down currents generated by or associated with intense convective activity and that produce marked changes in surface wind, temperature, and pressure. It can be measured rapidly and continuously with improved spatial and temporal resolution using remote sensing devices [22] involving electromagnetic and acoustic waves.

Sudden local variation of wind direction or speed (wind shear) in the lower atmosphere can be an unexpected and serious hazard to aircraft landing and take-off. SODAR offers a promising new technique for remotely measuring wind shear, turbulence, and wind velocity parameters in the lower atmosphere, information which can be of great help in saving hazardous situations in aviation.

Shear echoes form after subsiding thermal plumes (Figs. 14-17). It remains throughout the night, and in the morning, when the earth gets heated up by the sun, the shallow layer formed gets lifted and a thermal plume starts forming. SODAR visualises the changes in the pattern and height of the nighttime stable layer. In the case of shallow

layers, weather conditions have a clear effect. Layer with plain top formed in the low wind conditions or with no wind. Thickness of this layer increases if this condition persists. Surface wind brings mixing in the stable layer. The spikes on the structure show the gustiness of the wind. Sometimes a multilayered structure forms above the surface-based layer. The layers have features of sinusoidal motion in clear weather conditions and sharp vortices in turbulent weather conditions. The dot echo structure above the surface-based layer indicates water vapor. It is observed in moist conditions soon after rain or in the evenings in the rainy season [12,34].

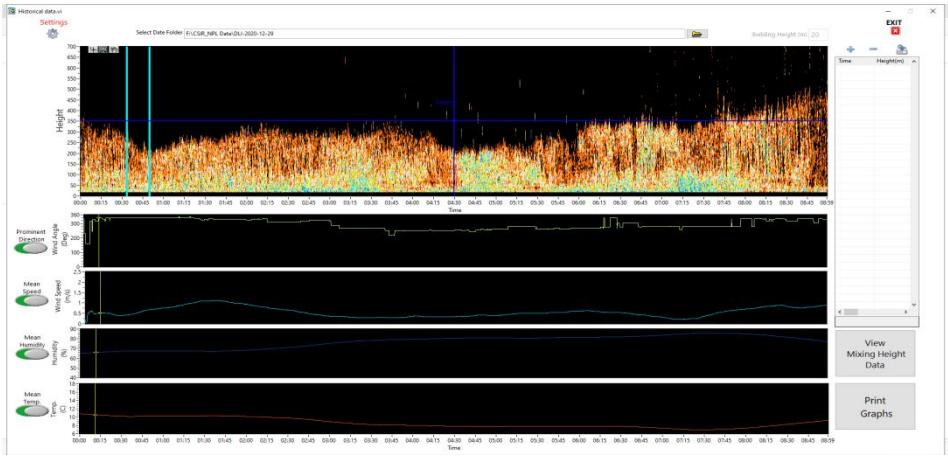

Fig. 14. Inversion with tall spiky (strong wind shear).

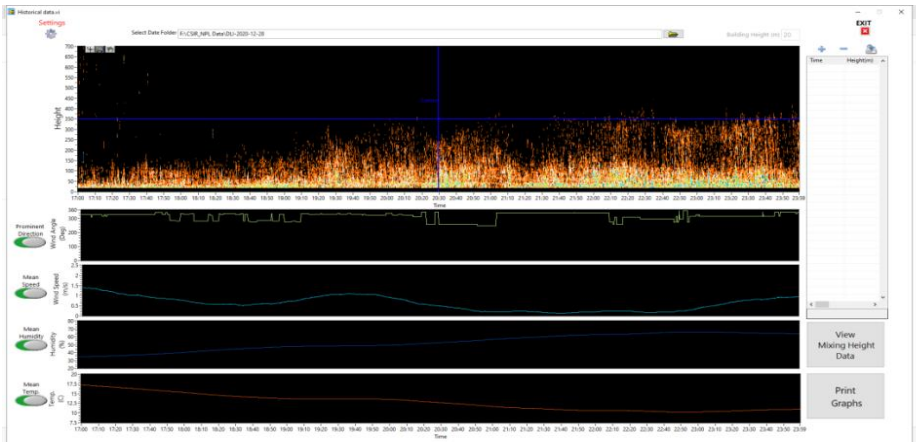

Fig. 15. Inversion with short spiky (strong wind weak inversion).

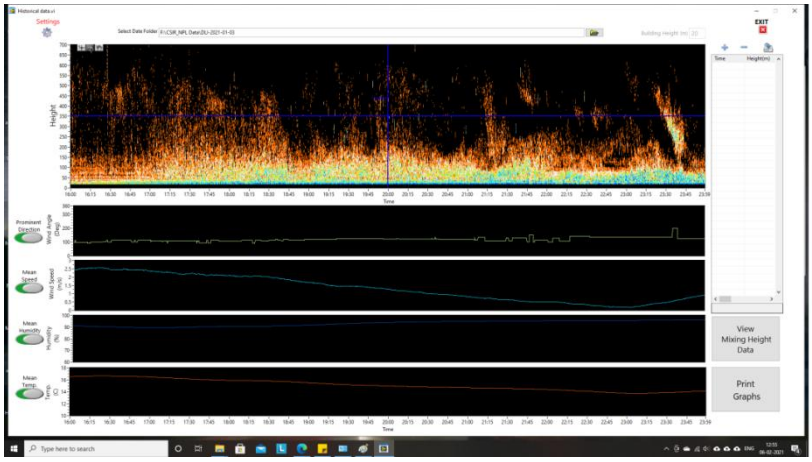

Fig. 16. Strong wind after rain.

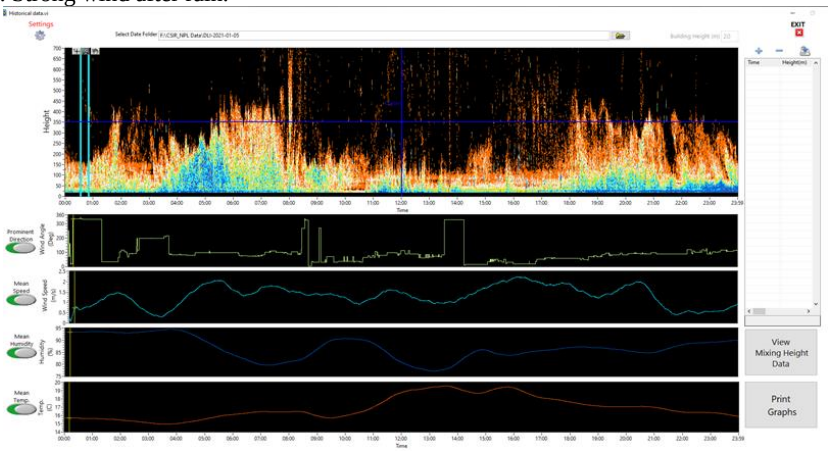

Fig. 17. Strong wind twenty-four hours.

4. Conclusion

SODAR has been found to provide a new and valuable tool for sensing temperature and velocity structure in the ABL. It is observed from the different structures that morning echograms represent a surface-based layer of statically stable air. Turbulence is formed in this layer due to solar heating of the surface air, and convective wind steadily builds up, forming a mixed boundary layer that gradually erodes the inversion upwards from the surface, increasing the depth of the mixed boundary layer. Similarly, surface-based stable layers, nonctural inversion with multi-layer structure, and stable layers with undulating structure are all examples of noctural structures. These echograms show convectively rising air packages in the shape of random spikes above the surface, elevated/multiple layers, and undulating reflecting layers. These nighttime recordings can be used to examine atmospheric mixing capacities in order to investigate the influence of a planned

airport on air pollution. Despite regular surface cooling and a steady temperature profile across the mixed region, a strong surface breeze caused mixing to a high elevation of roughly 500 m in the discussed echograms. These are wind-driven deep shear echoes on the ground. These are some wave features stacked aloft, as seen in the middle of the night, indicating shears. The data presented clearly shows that this technique has a lot of potential for meteorological research and operations. This potential stems from the capacity to feel the environment remotely using a relatively basic device at a high sampling rate and to assemble these samples in such a way that the average temperature structure can be examined in real time using a simple visual integration procedure.

Acknowledgment

This research was carried out at the CSIR-NPL. The authors are grateful to the Director of the CSIR National Physical Laboratory (NPL).

References

1. K. Soni, S. Kapoor, K. S. Parmar, and D. G. Kaskaoutis, Atmos. Res. **149**, 174 (2014). https://doi.org/10.1016/j.atmosres.2014.05.025
2. S. -E. Pena, Gryning, and A. N. Hahmann, JGR Atmos. **118**, 1924 (2013). https://doi.org/10.1002/jgrd.50175
3. J. Quan, X. Tie, Q. Zhang, Q. Liu, X. Li, Y. Gao, and D. Zhao, Atmos. Envir. **88**, 83 (2014). https://doi.org/10.1016/j.atmosenv.2014.01.058
4. S. Chandra, A. K Dwivedi, and M. Kumar, J. Earth Syst. Sci. **123**, 1233 (2014). https://doi.org/10.1007/s12040-014-0458-4
5. J. N. A. Aryee, L. K. Amekudzi, K. Preko, W. A. Atiah, and S. K. Danuor, Scientific Afr. **7**, 228 (2020).
6. S. Emeis, C. Munkel, S. Vogt, W. J. Muller, and K. Schafer, Atmos. Envir. **38**, 273 (2004).
7. S. Odintsov, E. Miller, A. Kamardin, I. Nevzorova, A. Troitsky, and M. Schröder, Environments **2021**, 115 (2021). https://doi.org/10.3390/environments8110115
8. T. J. Wagner, A. C. Czarnetzki, M. Christiansen, R. B. Pierce, C. O. Stanier, A. F. Dickens, and E. W. Eloranta, J. Atmos. Sci. 1005 (2022). https://doi.org/10.1175/JAS-D-20-0297.1
9. S. Emeis, in Handbook of Atmospheric Measurements (Springer, Cham, 2021) pp. 663-684.
10. A. Lammert and J. Bosenberg, Boundary-Layer Meteorol. **119**, 159 (2006). https://doi.org/10.1007/s10546-005-9020-x
11. B. Hennemuth and A. Lammert, Boundary-Layer Meteorol. **120**, 181 (2006). https://doi.org/10.1007/s10546-005-9035-3
12. N. Kumar, K. Soni, N. Garg, R. Agarwal, D. Saha, M. Singh, and G. Singh, Int. J. Remote Sensing **38**, 3466 (2017). https://doi.org/10.1080/01431161.2017.1294774
13. D. N. Asimakopoulos, C. G. Helmis, and J. Michopoulos, Meteorol. Atmos. Phys. **85**, 85 (2004). https://doi.org/10.1007/s00703-003-0036-9
14. N. Kumar, K. Soni, R. Agarwal, and M. Singh, J. Acoustical Soc. Am. **146**, 2997 (2019). https://doi.org/10.1121/1.5137378
15. N. Kumar, K. Soni, and R. Agarwal, Model. Earth Syst. Envir. **7**, 209 (2021). https://doi.org/10.1007/s40808-020-00872-0
16. R. L. Coulter and M. A. Kallistratova, Meteorol. Atmos. Phys. **85**, 3 (2004). https://doi.org/10.1007/s00703-003-0031-1
17. L. Xing-Sheng, J. E. Gaynor, and J. C. Kaimal, Boundary-Layer Meteorol. **26**, 157 (1983). https://doi.org/10.1007/BF00121540

18. N. Kumar, K. Soni and Agarwal, and R. Tellus, A: Dynamic Meteorol. Oceanography **73**, 1 (2021). https://doi.org/10.1080/16000870.2021.1926132
19. R. M. Hardesty, P. A. Mandics, D. W. Beran, and R. G. Strauch, Bull. Am. Met. Soc. **58**, 910 (1977). https://doi.org/10.1175/1520-0477(1977)058<0910:TDAAMR>2.0.CO;2
20. P. Chourey, K. Soni, N. J. Singh, and R. Agarwal, IETE J. Res. (2022). https://doi.org/10.1080/03772063.2022.2026826
21. N. Kumar, K. Soni and, R. Agarwal, MAPAN **36**, 785 (2021). https://doi.org/10.1007/s12647-021-00477-7
22. S. P. Singal, B. S. Gera, and S. K. Aggarwal, J. Sci. Industr. Res. **4**, 469 (1984).
23. S. P., Singal, B. S. Gera, and D. R. Pahwa, Int. J. Remote Sensing **15**, 427 (1994). https://doi.org/10.1080/01431169408954084
24. S. P. Singal, B. S. Gera, and S. K. Agarwal, Boundary-Layer Meteorol. **23**, 105 (1982). https://doi.org/10.1007/BF00116114
25. V. E. Derr and C. G. Little, Appl. Opt. **9**, 1976 (1970). https://doi.org/10.1364/AO.9.001976
26. V. Mohnan, B. S. Gera, N. Gera, and N. C. Gupta, Int. J. Sci. Eng. Res. **4**, 1634 (2013).
27. N. Gera, N. C. Gupta, V. Mohanan, and B. S. Gera, Int. J. Sci. Eng. Res. **4,** 1806 (2013).
28. M. N. Ferdous, M. A. Islam, P. Chakrabortty, and S. Kabir, J. Sci. Res. **13,** 707 (2021). https://doi.org/10.3329/jsr.v13i3.50647
29. M. R. Islam and S. H. Naqib, J. Sci. Res. **13**, 495 (2021). https://doi.org/10.3329/jsr.v13i2.50273
30. V. Lyulyukin, M. Kallistratova, D. Zaitseva, D. Kuznetsov, A. Artamonov, I. Repina, I. Petenko, R. Kouznetsov, and A. Pashkin, Atmosphere **10,** 811 (2019). https://doi.org/10.3390/atmos10120811
31. Singal, S. P., S. K. Aggarwal, and B. S. Gera. J. Met. Hydrol. Geophys. **28**, 39 (1977). https://doi.org/10.54302/mausam.v28i1.2658
32. N. Gera, N. C. Gupta, V. Mohanan, and B. S. Gera, Int. J. Sci. Eng. Res. **4**, 1634 (2013).
33. N. Gera, N. C. Gupta, V. Mohanan, and B. S. Gera, Int. J. Sci. Eng. Res. 4, 1805 (2013).
34. S. P. Singal, S. K. Aggarwal, and B. S. Gera, Mausam **33**, 439 (1982). https://doi.org/10.54302/mausam.v33i4.2592